ORIGINAL ARTICLE

Immunostimulatory gene therapy combined with checkpoint blockade reshapes tumor microenvironment and enhances ovarian cancer immunotherapy

Yunzhu Lin[a,b,†], Xiang Wang[c,†], Shi He[c], Zhongxin Duan[c], Yunchu Zhang[c], Xiaodong Sun[e], Yuzhu Hu[d,*], Yuanyuan Zhang[a,*], Zhiyong Qian[c], Xiang Gao[c,*], Zhirong Zhang[a]

[a]*Key Laboratory of Drug Targeting and Drug Delivery Systems, Ministry of Education, West China School of Pharmacy, Sichuan University, Chengdu 610041, China*
[b]*Department of Pharmacy, Evidence-based Pharmacy Center, West China Second University Hospital, Key Laboratory of Birth Defects and Related Diseases of Women and Children, Sichuan University, Chengdu 610041, China*
[c]*Department of Neurosurgery and Institute of Neurosurgery, State Key Laboratory of Biotherapy and Cancer Center, West China Hospital, West China Medical School, Sichuan University and Collaborative Innovation Center for Biotherapy, Chengdu 610041, China*
[d]*Department of Radiation Oncology, State Key Laboratory of Biotherapy and Cancer Center, West China Hospital, West China Medical School, Sichuan University and Collaborative Innovation Center for Biotherapy, Chengdu 610041, China*
[e]*West China School of Basic Medical Sciences & Forensic Medicine, Sichuan University, Chengdu 610041, China*

Abstract Immune evasion has made ovarian cancer notorious for its refractory features, making the development of immunotherapy highly appealing to ovarian cancer treatment. The immune-stimulating cytokine IL-12 exhibits excellent antitumor activities. However, IL-12 can induce IFN-γ release and subsequently upregulate PDL-1 expression on tumor cells. Therefore, the tumor-targeting folate-modified delivery system F-DPC is constructed for concurrent delivery of IL-12 encoding gene and small molecular PDL-1 inhibitor (iPDL-1) to reduce immune escape and boost anti-tumor immunity. The physicochemical

---

*Corresponding authors.

E-mail addresses: huyuzhu023@foxmail.com (Yuzhu Hu), zhangyy@scu.edu.cn (Yuanyuan Zhang), xianggao@scu.edu.cn (Xiang Gao).

[†]These authors made equal contributions to this work.

characteristics, gene transfection efficiency of the F-DPC nanoparticles in ovarian cancer cells are analyzed. The immune-modulation effects of combination therapy on different immune cells are also studied. Results show that compared with non-folate-modified vector, folate-modified F-DPC can improve the targeting of ovarian cancer and enhance the transfection efficiency of pIL-12. The underlying anti-tumor mechanisms include the regulation of T cells proliferation and activation, NK activation, macrophage polarization and DC maturation. The F-DPC/pIL-12/iPDL-1 complexes have shown outstanding antitumor effects and low toxicity in peritoneal model of ovarian cancer in mice. Taken together, our work provides new insights into ovarian cancer immunotherapy. Novel F-DPC/pIL-12/iPDL-1 complexes are revealed to exert prominent anti-tumor effect by modulating tumor immune micro-environment and preventing immune escape and might be a promising treatment option for ovarian cancer treatment.

1. Introduction

Ovarian cancer, the third most common gynecologic malignancies worldwide, accounts for 2.5% of all female malignancies[1,2]. Approximately 300,000 new cases of ovarian cancer were diagnosed and nearly 207,000 ovarian cancer-related deaths worldwide in 2020[3]. Surgery and chemotherapy are the primary treatment options for ovarian cancer, however, conventional surgery often fails to eradicate tumor cells, and chemotherapy suffers from defects such as drug resistance and high toxicity due to nonspecific tumor targeting[4−6]. Therefore, recurrence of ovarian cancer is clinically common, resulting in a high mortality rate. There is an urgent need to seek novel and more effective treatment strategies for ovarian cancer.

Immunotherapy is a popular cancer treatment strategy in recent years and has been clinically proven to be effective against a variety of malignant tumors[7]. Different from conventional therapies, cancer immunotherapy mainly activates the host immune system and enhances the recognition of tumor cells by immune cells, so as to eliminate tumor cells[8,9]. Cytokine therapy is one of the most promising immunotherapy strategies in cancer research[10]. Interleukin-12 (IL-12), a pleiotropic cytokine mainly produced by activated dendritic cells (DCs) and macrophages during T-cell initiation, consists of p35 chain and p40 chain[11]. IL-12 regulates innate and adaptive immunity and is considered as an ideal candidate for immunotherapy in a variety of tumors[12−19]. Previous studies have shown that IL-12 can not only enhance natural killer cell activity, but also has direct cytotoxicity, making it a potential therapeutic agent for ovarian cancer[20−22]. However, direct administration of recombinant IL-12 protein has shown undesirable systemic toxicity and lower than expected efficacy[23,24]. Therefore, the therapeutic strategy of local delivery of IL-12 expression gene at the tumor site may be less toxic and exert a more desirable anti-tumor effect.

Immune evasion is one of the leading causes of cancer treatment failure[25]. Programmed cell death (PD) pathway is the most intensively studied immune evasion-related pathway[26,27]. Activated T lymphocytes express PD-1 on cell surface, and tumor cells express the ligand PDL-1, which binds to PD-1 on activated T cells, thus inhibiting the anti-tumor immune response of effector T cells and escaping the attack of the host immune system[28]. Previous studies have reported up-regulated expression of PDL-1 in epithelial ovarian cancer, which may lead to immune evasion[29]. Moreover, IL-12 can promote lymphocyte secretion of IFN-γ, subsequently inducing over-expre-

ssion of PDL-1 on tumor cells. Interrupting the interaction between PD-1 and PD-L1 with iPDL-1 enhances the ability of immune cells to recognize antigens on the surface of tumor cells. Thereupon, IL-12 combined with iPDL-1 is expected to become a potent immunotherapy approach for ovarian cancer, overcoming these obstacles and inducing synergistic anti-tumor effects.

Efficient vector systems is required to achieve tumor targeted gene and drug delivery. Non-viral vector systems are characterized by good physical stability, strong drug loading capacity and high encapsulation rate, and possess unique advantages in gene delivery[30−32]. Recent studies indicate that the immune escape generated by tumor cells leads to local rather than systemic immunosuppression, especially in solid tumors[33,34]. Therefore, targeted delivery of drugs to the tumor site is critical to improve therapeutic efficacy and reduce the risk of adverse events (AEs). Folate receptor (FR) is a glycoprotein located on the cell surface with a high affinity for folate (FA)[35]. FR is highly expressed in some epithelial cell-derived tumors, including ovarian cancer, but rarely expressed in most normal tissues, making it an attractive target for ovarian cancer therapy[36,37].

Herein, we construct a novel targeted nano-delivery F-DPC system consisting of FA-PEG-PCL copolymer, PEG-PCL copolymer and DOTAP, to load immunostimulatory gene and immune checkpoint small molecular inhibitor for ovarian cancer immunotherapy (Scheme 1). The gene and drug loaded complexes can be taken up by cancer cells overexpressing FRs and enters the cytoplasm through endocytosis. Then, pIL-12 escape from lysosomes and enter the nucleus to express IL-12 at tumor site, subsequently stimulating the proliferation and activation of T lymphocyte, promoting maturation of dendritic cells (DCs), and inhibiting M2 polarization of macrophages in tumor. Thereafter, increased lymphocyte secretion of IFN-γ induces overexpression of PDL-1 on tumor cells. The iPDL-1 binds to PDL-1 to enable activated T lymphocytes to recognize tumor cells, thus remodeling the immunosuppressive tumor microenvironment (TME) to restore antitumor immunity and prevent immune escape. Our research may provide a promising immunotherapeutic strategy for ovarian cancer.

2. Materials and methods

2.1. Materials and reagents

Folate (FA), monomethoxy poly (ethylene glycol) (MPEG), ε-CL and 3-(4,5-dimethylthiazol-2-yl)-2,5-diphenyl tetrazolium
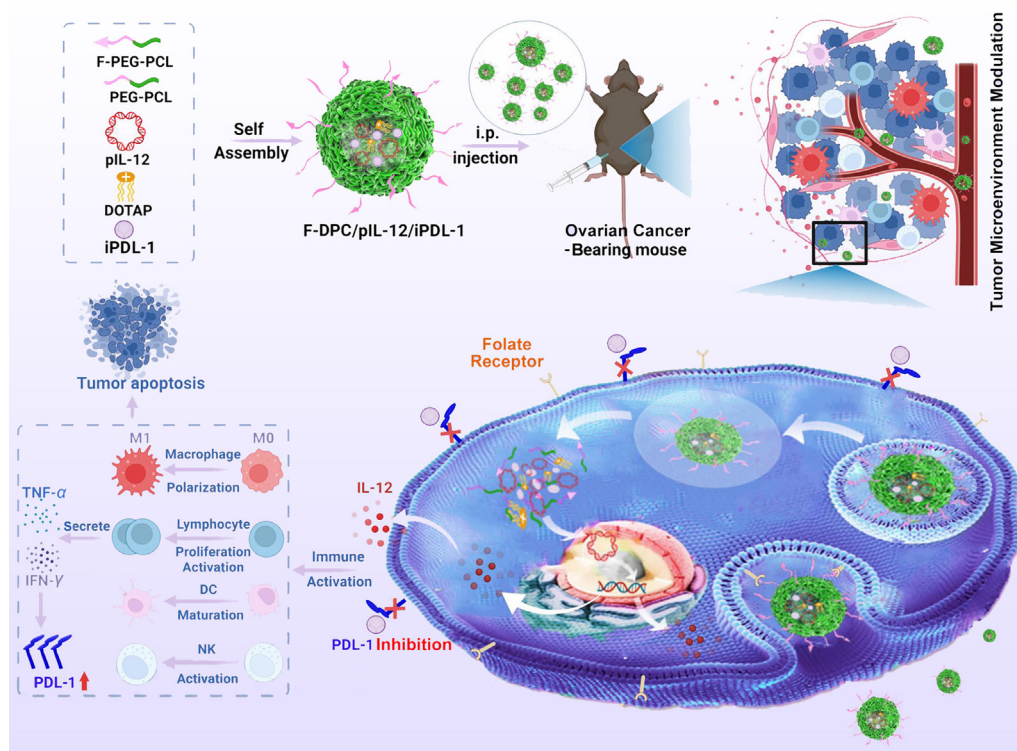
Scheme 1 Schematic representation of the folate receptor targeting F-DPC complexes for pIL-12 and iPDL-1 delivery. Combination therapy effectively modulates the tumor microenvironment and exhibits impressive antitumor effects in ovarian cancer treatment.

bromide (MTT) were purchased from Sigma−Aldrich (Darmstadt, Germany). 1,2-Dioleoyl-3-trimethylammonium-propane (DOTAP) was purchased from Avanti Polar Lipids (AL, USA). Dulbecco's modified Eagle's medium (DMEM) and fetal bovine serum (FBS) were both purchased from Gibco (NY, USA). The antibodies used in this study were summarized: rat anti-mouse CD31 polyclonal antibody, rat anti-mouse Ki67 polyclonal antibody, rat anti-mouse horseradish peroxidase (HRP)-conjugated secondary antibody (Servicebio, Wuhan, China); The anti-CD4 antibody, anti-CD8 antibody, anti-CD69 antibody, anti-CD11c antibody, anti-CD80 antibody, anti-CD86 antibody, anti-MHCII antiobody, anti-CD45 antibody, anti-CD11b antibody and anti-IFN-γ antibody (BD Pharmingen, NJ, USA); The anti-CD11b antibody, anti-CD206 antibody, anti-F480 antibody, anti-CD107a antibody, anti-CD49b antibody, anti-CD274 (PDL-1) antibody (Biolegend, CA, USA). The pvax and pIL-12 were extracted and purified using a QIAGEN Endofree Plasmid Mega Kit (Hulsterweg, Netherlands). The contents of murine IFN-γ, TNF-α and IL-12 p70 were detected by corresponding ELISA kits from Invitrogen (CA, USA).7-AAD/Annexin-V apoptosis kit was purchased from BD, Pharmingen (CA, USA).

2.2.   Synthesis and characterization of F-DPC/pIL-12/iPDL-1

The mixture of 10 g $MPEG_{2k}$, 10 g ε-caprolactone (ε-CL), and 0.1 g $Sn(Oct)_2$ were added into a round reaction flask and kept at 140 °C for 12 h to synthesize the MPEG-PCL diblock polymer. Then, 1.44 g of dicyclohexylmethane-4,4′-diisocyanate (HMDI) (5.49 mmol, −OH:−NCO = 1:1.1) was added as a crosslinking agent, and the reaction system was continuously stirred at 80 °C

for 8 h. After vacumm evaporation, the copolymers were successively dissolved in dichloromethane and precipitated in ice-cold diethyl ether. Ultimately, the obtained product was purified by dialysis and lyophilized for further use.

To prepare the F-DPC/pIL-12/iPDL-1 complexes, 15 mg FA-PEG-PCL, 75 mg PEG-PCL, 5 mg DOTAP and 5 mg iPDL-1 inhibitor (BMS-1, MedChemExpress, NJ, USA) were dissolved into 2 mL acetone, followed by vacuum evaporation at 55 °C water bath for 20 min. Subsequently, the formed film was dispersed in 5% glucose solution (GS) to obtain the F-DPC/iPDL-1. Meanwhile, the DPC/iPDL-1 complexes was prepared with the same method. The 5% GS suspension containing F-DPC/iPDL-1 or DPC/iPDL-1 nanoparticle and pDNA were gently mixed and incubated for 20 min to form the F-DPC/pIL-12/iPDL-1 or DPC/pIL-12/iPDL-1 complexes, respectively. The morphology of the F-DPC/pIL-12/iPDL-1 complexes was identified by transmission electron microscopy (TEM, FEI Tecnai G2 F20, USA). The particle size distribution and the zeta potential of the F-DPC/pIL-12/iPDL-1 complexes were determined by the NanoBrook particle size analyzer (Brookhaven Instruments, NY, USA).

2.3.   Transfection efficiency

For assessing the gene transfection efficiency, the nanoparticles and the plasmids encoding green fluorescent protein (pGFP) (5 μg) were separately dispersed in 500 μL of the DMEM medium. The medium containing pEGFP was slowly added to the medium containing nanoparticles and mixed well for 20 min. Then, the culture medium of ID8 cells were replaced by the mixed medium and incubated for 4 h. Subsequently, fresh culture

medium was supplemented and incubated for 48 h. The expression of GFP in transfected ID8 cells were identified using a fluorescent microscope (Olympus, Japan), and were semiquantitatively determined by flow cytometry (ACEA NovoCyte™, CA, USA).

2.4. Immune cells stimulation assay

With the aim to evaluate the impact of F-DPC/pIL-12/iPDL-1 nanocomposite transfection of tumor cells on immune cells, murine spleen derived lymphocytes, bone marrow-derived macrophages and bone marrow-derived DCs were isolated and stimulated with the supernatant of transfected ID8 cells respectively for 48 h. Then, the lymphocytes were stained with anti-CD4, anti-CD8, anti-CD69, and anti-IFN-γ antibodies for investigating the activation of lymphocytes. The proliferation status of lymphocytes was measured using the CCK-8 assay (Sigma Aldrich, Darmstadt, Germany). The macrophages were stained with anti-CD45, anti-CD11b, anti-F4/80, and anti-CD206 antibodies for detecting the M2 polarization of macrophages, and the DCs were stained with anti-CD11c, anti-CD80, anti-CD86 and anti-MHCII antibodies for analyzing DCs maturation. All stained cells were analyzed by flow cytometry. In addition, the secretion level of TNF-α and IFN-γ in the supernatant of immune cells were detected by ELISA method. Furthermore, the supernatant of stimulated lymphocyte was reversely applied to ID8 cells for 24 h incubation, followed by detection of the ID8 cells viability using CCK-8 assay.

2.5. In vivo antitumor efficacy evaluation

The mice model of abdominal ovarian cancer was established by intraperitoneal injection of 5×10^6 ID8 cells. Two weeks after tumor inoculation, the tumor-bearing mice were randomly allocated into seven groups and received corresponding treatment by intraperitoneal injection: (A) Untreated; (B) F-DPC nanoparticles (vehicle); (C) F-DPC/pvax; (D) iPDL-1; (E) F-DPC/pIL-12; (F) DPC/pIL-12/iPDL-1;(G) F-DPC/pIL-12/iPDL-1. The dosage of pIL-12 or pvax was 20 μg per mouse. The treatment plan is twice a week, for a total of twelve times. During the treatment schedule, the body weight of mice was continuously monitored and recorded. At the endpoint, the serum, tumor nodules, ascites and vital organs of mice were collected and processed for subsequent study. Moreover, the expression levels of IL-12, TNF-α and IFN-γ in serum, ascites and tumor tissues were quantified by ELISA assay.

2.6. Immunomodulation effect in vivo

To explore the changes of immune cells in TME after various treatment, the tumor modules, ascites and spleens from experimental mice were harvested and prepared into single-cell suspension. Then, the samples were stained with fluorescence-conjugated antibodies for analyzing lymphocytes activation as well as natural killer (NK) cells activation. The stained cell samples were analyzed by flow cytometry.

2.7. Effect on tumor proliferation and angiogenesis

Immunohistochemical and immunofluorescence staining were performed on tumor sections to explore the effect of different treatment on tumor proliferation and angiogenesis. The immunohistochemical staining of Ki67 and CD31 were carried out according to our previous research. All the stained tumor sections were observed under a light microscope (Leica, Wetzlar, Germany) and the
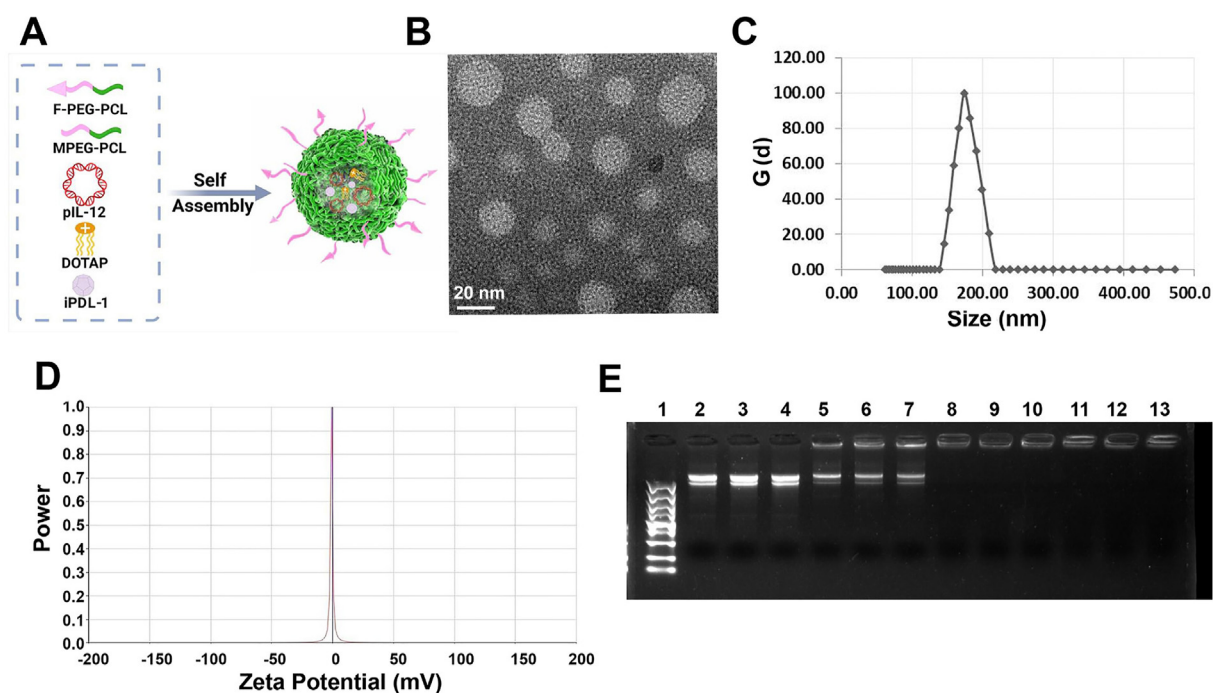

Figure 1 Characteristics of F-DPC/pIL-12/iPDL-1 complexes. (A) The structure model of F-DPC/pIL-12/iPDL-1 complexes. (B) Morphological characteristics of F-DPC/pIL-12/iPDL-1 by TEM observation (scale bar = 20 nm). (C) Particle sizes distribution of F-DPC/pIL-12/iPDL-1 complexes. (D) Zeta-potential of F-DPC/pIL-12/iPDL-1 complexes. (E) Agarose gel electrophoresis assay of F-DPC nanoparticles loading pIL-12. Lanes 2−4, bare pIL-12; lanes 5−13, different mass ratios of pIL-12 with F-DPC nanoparticles (lanes 5−7, 1:12.5; lanes 8−10, 1:25; lanes 11−13, 1:50).

positively stained cells in five randomly selected areas were quantitatively analyzed.

2.8. Safety assessment

For drug safety evaluation, important serological biochemical indicators in treated mice were detected using a biochemical analyzer (Roche, Basel, Switzerland). Moreover, vital organs including heart, liver, spleen, lung and kidney were prepared as paraffin embedded tissue sections and applied for H&E staining. The stained sections were examined by two independent pathologists to identify organ histological morphology and distinguish pathological changes among different treatment groups.

2.9. Statistical analysis

The statistical analysis in the study were carried out using Graphpad Prism software v7.0 (CA, USA). For two groups comparison, Student's t-test was adopted, while for multiple comparisons, one-way ANOVA analysis was used. All the results were shown as a mean $\pm$ standard error of measurement (SEM). The P value < 0.05 was considered statistically significant at ($^*P < 0.05$, $^{**}P < 0.01$, $^{***}P < 0.001$, $^{****}P < 0.0001$).

3. Results and discussion

3.1. Preparation and characterization of tumor-targeting F-DPC/pIL-12/iPDL-1

Commonly-used gene delivery systems include viral and non-viral vectors[38]. However, the low safety, limited gene load, high immunogenicity, and difficulty in preparation restricted the clinical application of viral vectors. In this study, non-viral PEG-PCL copolymers were synthesized by hydrophilic PEG and hydrophobic PCL with high chemical stability, long circulation and biodegradability[39]. Moreover, FA modification confers tumor targeting capabilities on PEG-PCL copolymers. The PEG-PCL and FA-PEG-PCL copolymers were successfully synthesized (Supporting Information Figs. S1 and S2). FA-PEG-PCL, PEG-PCL, DOTAP, pIL-12 and iPDL-1 corporately formed a core−shell structure by self-assembly. The core consists of the hydrophobic part of the PCL segment and the hydrophobic tail of DOTAP, and the hydrophobic small molecule PDL-1 inhibitor is also loaded in the hydrophobic core. The outer shell is mainly composed of hydrophilic PEG segment, which contributes to the structural stability of the nanocomposite. Moreover, the positive charge possessed by DOTAP can effectively attract pIL-12 through electrostatic interactions. The structural model of the F-DPC/pIL-12/iPDL-1 complexes is shown in Fig. 1A.

The spherical structure of the F-DPC/pIL-12/iPDL-1 complexes was demonstrated by TEM observation (Fig. 1B). According to DLS assay, the average diameter of the F-DPC/pIL-12/iPDL-1 complexes was about 182.9 nm and the zeta potential was approximately 0 mV (Fig. 1C and D), indicating that the F-DPC/pIL-12/iPDL-1 composite was nearly electrically neutral. The gene encapsulation capacity of F-DPC nanoparticles was analyzed by agarose gel electrophoresis. The bare plasmid showed bright bands (Lanes 2−4), and the plasmid displacement was partially restained (Lanes 7) when the mass ratio of pIL-12 to F-DPC was 1:12.5. When the mass ratio of pIL-12 to F-DPC is greater than 1:25 (Lanes 10, 1:25; Lanes 113, 1:50) (Fig. 1E), the plasmid migration was completely retarded, suggesting that IL-12 plasmid was fully encapsulated by F-DPC nanoparticles.
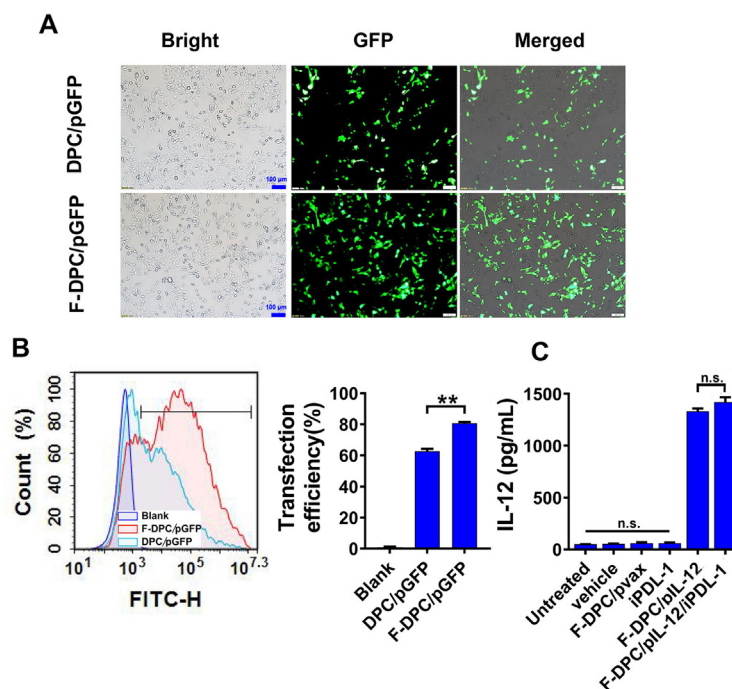

Figure 2 Gene transfection efficiency of F-DPC/GFP in ovarican cancer cells. (A) Representative images of GFP expression in ID8 cells (Scale bar = 100 μm). (B) The transfection efficiency measured by flow cytometry. (C) The secretion level of IL-12 from ID8 cells by ELISA. Data are presented as mean $\pm$ SEM ($n = 3$). $^*P < 0.05$, $^{**}P < 0.01$, $^{***}P < 0.001$, ns, not significant.

3.2. F-DPC efficiently delivered pDNA into tumor cells

Previous clinical trials revealed that the administration of recombinant cytokine IL-12 failed to achieve the expected antitumor effect due to insufficient concentrations in the tumor, yet adversely evoked a dose-related severe toxic response[40,41]. Hence, targeted delivery of IL-12 expression gene into ovarian cancer cells through a vector system is an ideal approach to stimulate anti-tumor immune response and avoid systemic toxicity[42,43]. The successful transfection of IL-12 expression gene into cells is crucial for subsequent expression of the IL-12 protein. Therefore, we explored the intracellular localization of F-DPC/pIL-12/iPDL-1 in ID8 cells by time-lapse confocal microscopy (Supporting Information Fig. S3). Serial tracer analysis (0.5, 1, 3 and 5 h) showed that pIL-12 labeled with green fluorescent dye YOYO-1 delivered

by F-DPC was initially co-localized with lysosomes in the cytoplasm. Subsequently, pIL-12 escaped from the lysosome and eventually entered the nucleus, as demonstrated by the almost complete overlap of YOYO-1-labeled pIL-12 and the nucleus, indicating the lysosomal escape ability of the F-DPC/pIL-12/iPDL-1 complexes.

High transfection efficiency is a prerequisite for effective gene therapy. The hydrophobic core of the micelle provided spaces for insoluble small molecule drugs, while the positively charged cationic DOTAP could further compress the particle size through electrostatic interactions with negatively charged nucleic acids[44], endowing the vector system with high drug and gene delivery efficiency. Moreover, FR is highly expressed in epithelial ovarian cancers and positively correlated with the stage and grade of tumor, and its expression level is not affected by chemotherapeutic
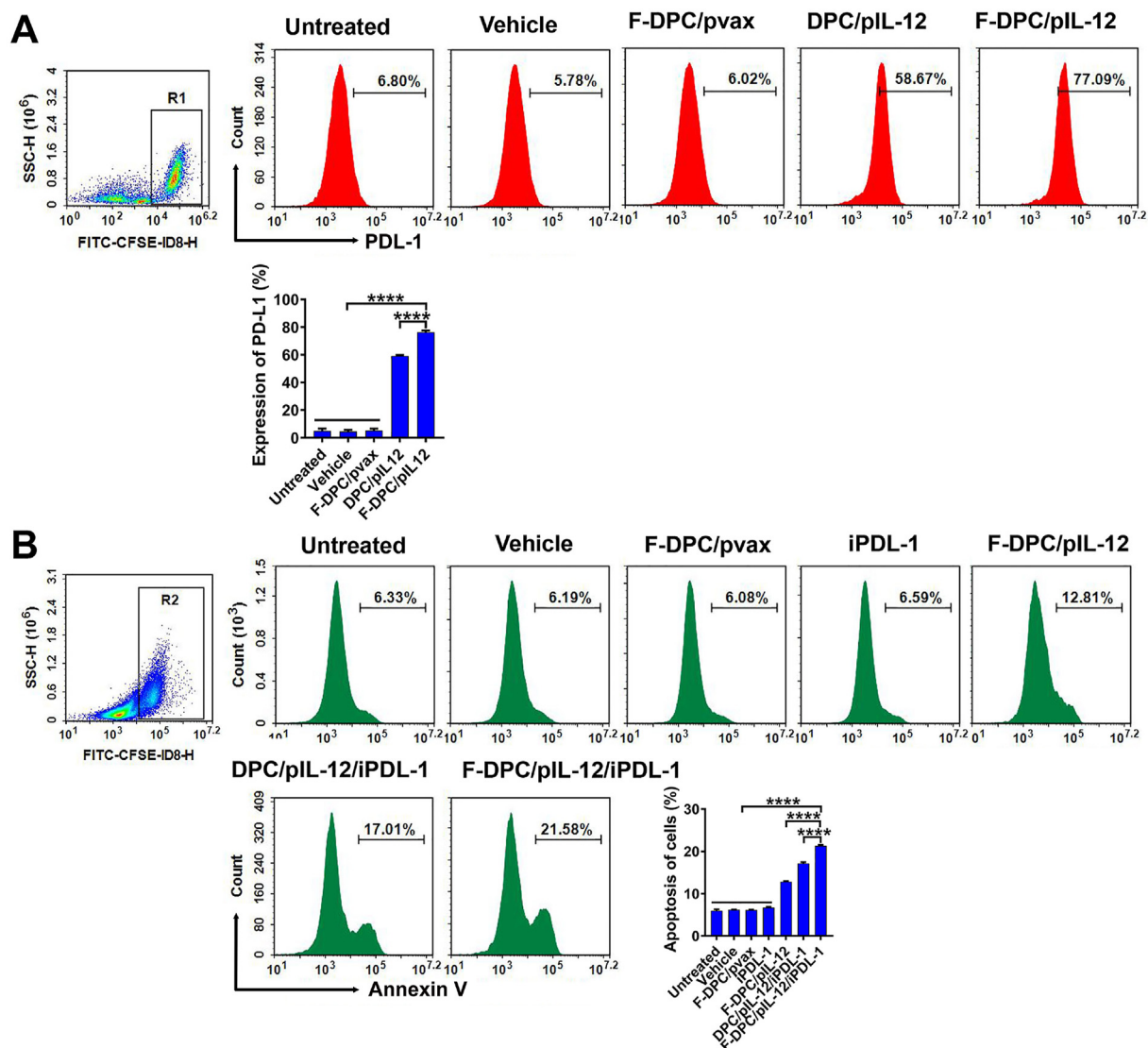

Figure 3 Increased PDL-1 expression and promoted apoptosis of ID8 cells. (A) Expression of PDL-1 on ID8 cells was detected by flow cytometry. The supernatant from transfected cells was collected to stimulate lymphocytes, and then the lymphocytes culture medium was harvested to incubate tumor cells. The expression of PDL-1 on ID8 cells in each treatment group was analyzed using flow cytometry. Data are presented as mean ± SEM ($n = 3$). ****$P < 0.0001$. (B) Apoptosis of ID8 cells was detected by flow cytometry. We transfected the CFSE-labeled tumor cells with different complexeses and added lymphocytes for co-incubation for 48 h. The apoptosis of tumor cells using PE-Annexin V staining method was subsequently analyzed. Data are presented as mean ± SEM ($n = 3$). ****$P < 0.0001$.

drugs, with FR expression remaining high after neoadjuvant chemotherapy for ovarian cancer[37,45,46]. Therefore, we modified the PEG-PCL copolymers with FA to enhance drug accumulation at the ovarian tumor site and reduce off-target effects. The transfection efficiency of F-DPC complexes and DPC complexes in ID8 cells were identified by transfecting plasmid encoding green fluorescent protein (pGFP), respectively. After 24 h of transfection, large numbers of GFP-positive cells were observed in the F-DPC/pGFP group and the DPC/pGFP group. The GFP expression was higher in ID8 cells transfected with F-DPC/pGFP compared with that transfected with DPC/pGFP (Fig. 2A). The gene transfection efficiency in ID8 cells was further examined by flow cytometry, and similar results were observed (Fig. 2B). After 24 h transfection, the transfection efficiency was approximately 80% in the F-DPC/pGFP group and about 60% in the DPC/pGFP group, indicating higher *in vitro* transfection efficiency of F-DPC than that of DPC. Furthermore, we detect the IL-12 expression

levels in the supernatants using ELISA assay after 24 h transfection. The results showed that both DPC/pIL-12/iPDL-1 and F-DPC/pIL-12/iPDL-1 groups had high IL-12 secretion, and F-DPC/iPDL-1/pIL-12 complexes could significantly improve IL-12 secretion compared with DPC/pIL-12/iPDL-1 complexes (Fig. 2C). These results further demonstrate that F-DPC can deliver pIL-12 more effectively into tumor cells.

3.3. Increased PDL-1 expression and promoted apoptosis in ID8 cells by F-DPC/pIL-12/iPDL-1

Previous study revealed that IL-12 could result in IFN-γ secretion from lymphocytes, subsequently inducing upregulated expression of PDL-1 on tumor cells[47]. To identify the PDL-1 expression on tumor cells, we collected the supernatant derived from transfected cells to stimulate lymphocytes, and then the lymphocytes culture medium was harvested to reversely incubate tumor cells. The
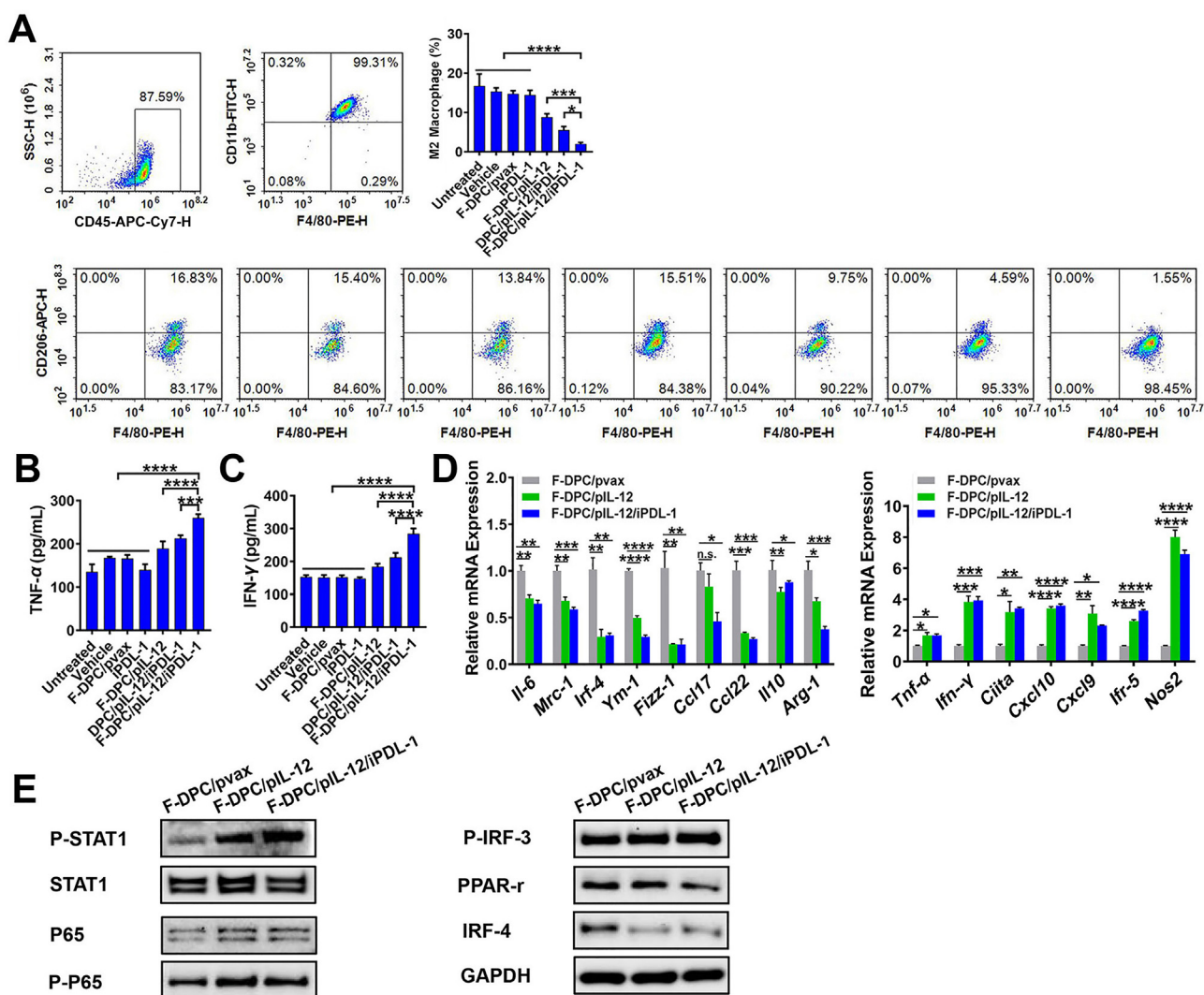

Figure 4 Polarization of macrophages *in vitro*. (A) After being stimulated by the supernatants from transfected ID8 cells for 48 h, the polarization status of macrophages *in vitro* was analyzed by flow cytometry. The secretion levels of TNF-α (B) and IFN-γ (C) from stimulated macrophages were measured by ELISA. (D) The mRNA levels of immunosuppressive M2 phenotype-related genes (left) and proinflammatory M1 phenotype-related genes (right) in stimulated macrophages were detected by RT-PCR. Data are presented as mean ± SEM (n = 3). *P < 0.05; **P < 0.01, ***P < 0.001, ****P < 0.0001. (E) Protein levels in the macrophages stimulated by supernatants from F-DPC/pvax, F-DPC/pIL-12, or F-DPC/pIL-12/iPDL-1 transfected ID8 cells were analyzed by Western blot.

expression of PDL-1 on ID8 cells was significantly increased in F-DPC/pIL-12 group and DPC/pIL-12 group, which reached 77.09% and 58.67%, respectively (Fig. 3A). These results indicated that F-DPC/pIL-12 can enhance the secretion of IL-12, further induce more expression of PDL-1 on tumor cells, leading to immune escape. One essential strategy for cancer immunotherapy is "immune normalization", which is unblocking immune responses and selectively regulating immunity in the TME based on immune escape mechanisms[35,48]. The anti-PD-1/PDL-1 pathway is by far the most explicit representative of the "immune normalization" strategy, and many drugs against this pathway have been marketed and proven effective in improving the antitumor immune response against multiple tumor types[35]. It is thus speculated that combined application of immune checkpoint inhibitor will be beneficial to improve the immunosuppressive state of TME and enhance the efficacy of immunotherapy. We transfected the CFSE-labeled tumor cells with different complexeses and added lymphocytes for co-incubation for 48 h. The apoptosis of tumor cells was analyzed using PE-Annexin V staining. The flow cytometry result revealed that F-DPC/pIL-12/iPDL-1, DPC/pIL-12/iPD-L1, F-DPC/pIL-12, iPDL-1, F-DPC/pvax, F-DPC (vehicle), and Control group exhibited apoptotic cell rates of 21.58%, 17.01%, 12.81%, 6.59%, 6.08%, 6.19%, and 6.33%, respectively. F-DPC/pIL-12/iPDL-1 group showed the highest apoptosis rate among all groups (Fig. 3B), indicating the simultaneous delivery of both pIL-12 and iPDL-1 with F-DPC could significantly enhance the antitumor effect.

3.4. F-DPC/pIL-12/iPDL-1 modulated the M1/M2 polarization status of macrophages

It is hypothesized that the antitumor ability of F-DPC/IL-12/iPDL-1 is mainly through the modulation of tumor immune micr-oenvironment. Therefore, the states of macrophage polarization, DC maturation, and T lymphocyte activation were studied. Firstly, we collected the supernatants of ID8 cells from each group to stimulate the bone marrow derived macrophages and stained the cells with anti-CD45, anti-CD11b, anti-F4/80, anti-CD206 antibodies to identify the polarization status. Results showed that the percentages of $CD45^+CD11b^+F4/80^+CD206^{high}$ cells in F-DPC/pIL-12/iPDL-1, DPC/pIL-12/iPDL-1, F-DPC/pIL-12, iPDL-1, F-DPC/pvax, F-DPC (vehicle) and control group (Untreated) were 1.55%, 4.59%, 9.75%, 15.51%, 13.84%, 15.40% and 16.83%, respectively. These results demonstrated that F-DPC/pIL-12/iPDL-1 treatment significantly reduced the polarization of macrophages to the tumor-associated M2 phenotype (Fig. 4A).

TNF-α and IFN-γ can mediate both innate and adaptive immune responses and are important pro-inflammatory cytokines for tumor eradication[49]. Our results showed that the supernatant from F-DPC/pIL-12/iPDL-1 transfected ID8 cells could significantly promote the secretion of TNF-α and IFN-γ by macrophages (Fig. 4B and C). Next, we assessed the expression levels of representative immunosuppression-related and proinflammatory-related genes in macrophages using RT-PCR. After macrophages stimulated with the supernatants from transfected ID8 cells, the
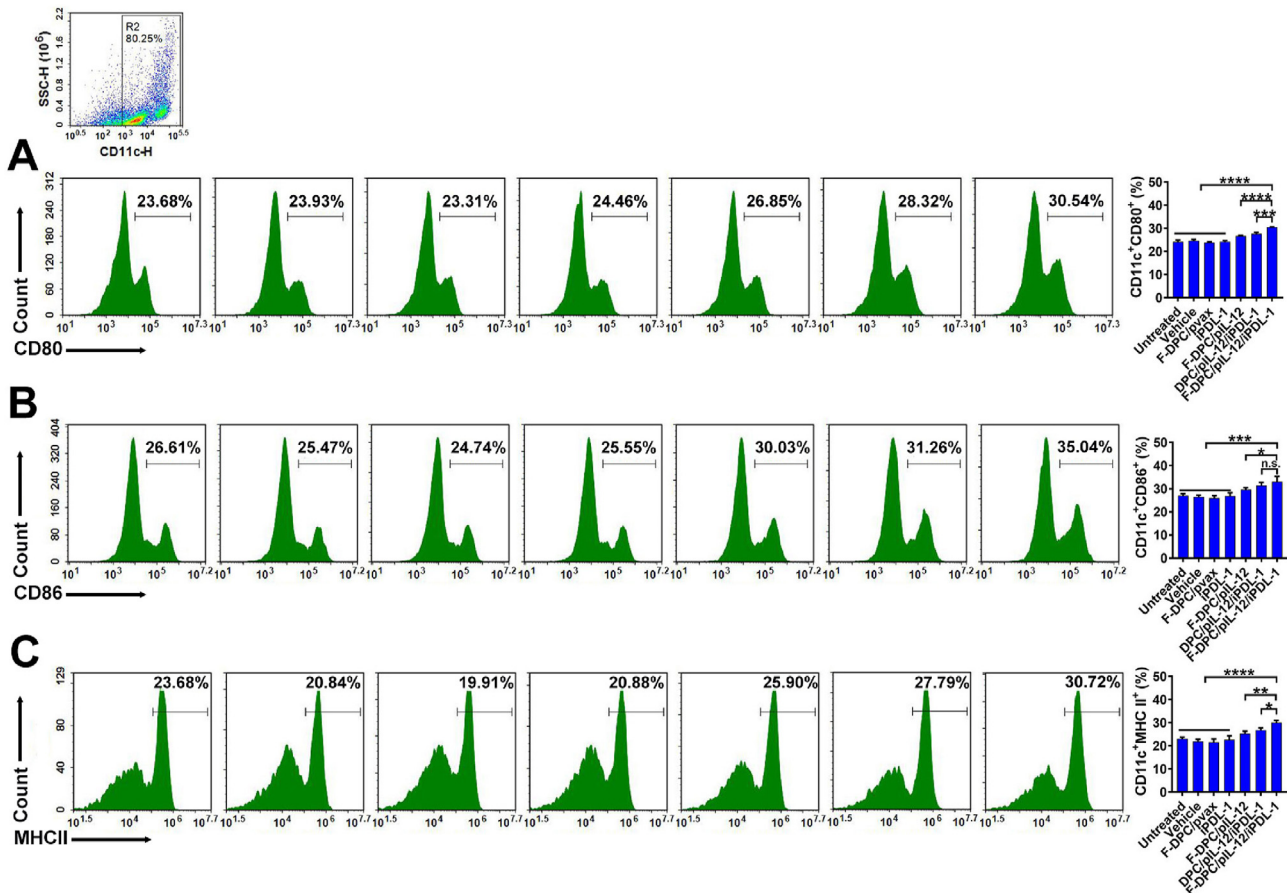

Figure 5 Promoted maturation of DCs *in vitro*. After being stimulated by the supernatants from transfected ID8 cells for 48 h, the relative percentages of DCs maturation markers were analyzed by flow cytometry (A, CD80, B, CD86, C, MHCII). Data are presented as mean ± SEM (*n* = 3). *P < 0.05; **P < 0.01, ***P < 0.001, ****P < 0.0001.
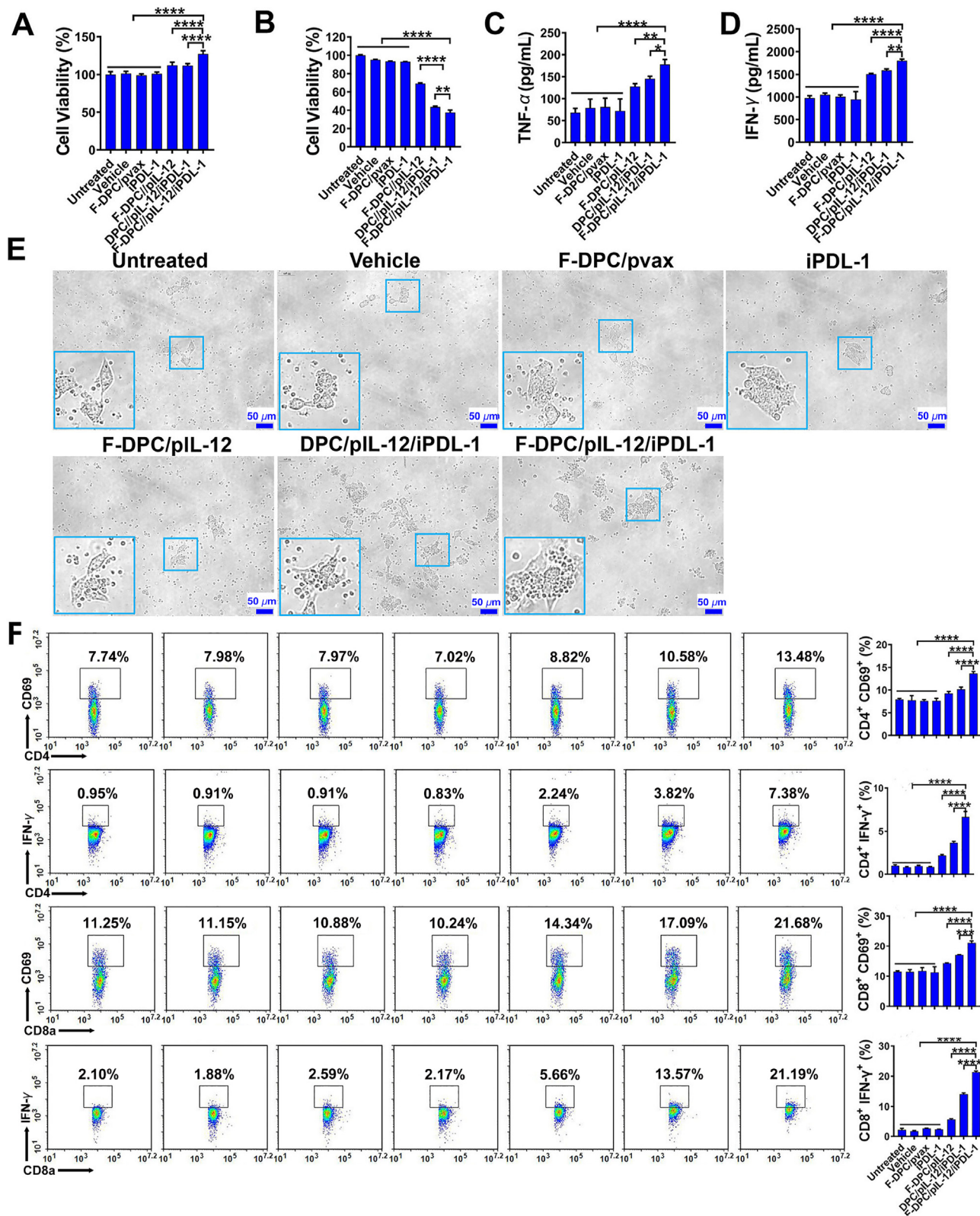
Figure 6 Increased proliferation and activation of lymphocytes boost tumor killing capability. (A) The lymphocytes were stimulated by supernatants from transfected tumor cells and analyzed by CCK-8. (B) The supernatants from stimulated lymphocytes were used to incubate ID8 cells for 48 h, and then the cell viability of ID8 cells was measured by CCK-8. The secretion levels of TNF-α (C) and IFN-γ (D) from lymphocytes were measured by ELISA. (E) The tumor cells besieged by lymphocytes were observed under a light microscope. (F) The proportions of activated lymphocytes subsets were determined by flow cytometry. Data are presented as mean $\pm$ SEM ($n = 3$). ***$P < 0.001$, ****$P < 0.0001$.

expression levels of immunosuppression-related genes (*Il-6*, *Mrc1*, *Irf4*, *Ym-1*, *Fizz1*, *Ccl17*, *Ccl22*, *Il-10*, *Arg-1*) were all significantly downregulated, while inflammation-related genes (*Tnf-α*, *Ifn-γ*, *Ciita*, *Cxcl10*, *Cxcl9*, *Irf-5*, *Nos2*) were significantly upregulated (Fig. 4D), indicating restrained immune suppression and strengthened antitumor immunity. Activation of STAT1 plays a crucial role in promoting M1 polarization of macrophages[50]. As shown in Fig. 4E, in macrophages stimulated by supernatants from F-DPC/pIL-12 and F-DPC/pIL-12/iPDL-1 transfected ID8 cells, the STAT1 pathway was markedly activated, with increased levels of protein P-STAT1, P-P65, and P-IRF3 and decreased levels of protein IRF4 and PPAR-γ. Taken together, these results suggest that IL-12 secreted by ID8 cells after F-DPC/pIL-12/iPDL-1 transfection can effectively inhibit macrophage M2 polarization and promote macrophage M1 polarization through activation of STAT1 pathway (Fig. 4E).

3.5. F-DPC/pIL-12/iPDL-1 treatment stimulated the maturation of DCs

Dendritic cells (DCs) play an critical role in antitumor immune response by processing and presenting tumor antigens to T cells[51]. Thus, we assessed the maturation of DCs by measuring the expression of co-stimulatory molecules including CD80, CD86 and MHCII. As seen in Fig. 5, after being stimulated with supernatant from transfected ID8 cells, higher proportions of CD11c^{+}CD80^{+}, CD11c^{+}CD86^{+} and CD11c^{+}MHCII^{+} DC cells were detected in the F-DPC/pIL-12/iPDL-1 group and DPC/pIL-12/iPDL-1 group than that in the F-DPC/pIL-12 group. These results indicate that the F-DPC/pIL-12/iPDL-1 and DPC/pIL-12/iPDL-1 can significantly promote the maturation of DCs and the F-DPC/pIL-12/iPDL-1 exhibited superior effect (Fig. 5A−C).

3.6. F-DPC/pIL-12/iPDL-1 strengthened lymphocytes activation and their killing capability against tumor cells

IL-12 can stimulate the proliferation of NK cells and cytotoxic T lymphocytes, and increase their cytotoxicity, as well as being the most potent stimulator for IFN-γ production by lymphocytes[41,49,52,53]. It can also induce immune memory against tumor and has significant antitumor effects in multiple pre-clinical models, and has shown moderate efficacy in cutaneous T-cell lymphoma (CTCL), Hodgkin and non- Hodgkin's lymphoma, as well as Kaposi's sarcoma in some small-sized, non-randomized clinical trials[40,41].

Therefore, the supernatants of ID8 cells after transfection were collected to stimulate the spleen derived lymphocytes. The lymphocyte viability was evaluated by the CCK-8 method, and the
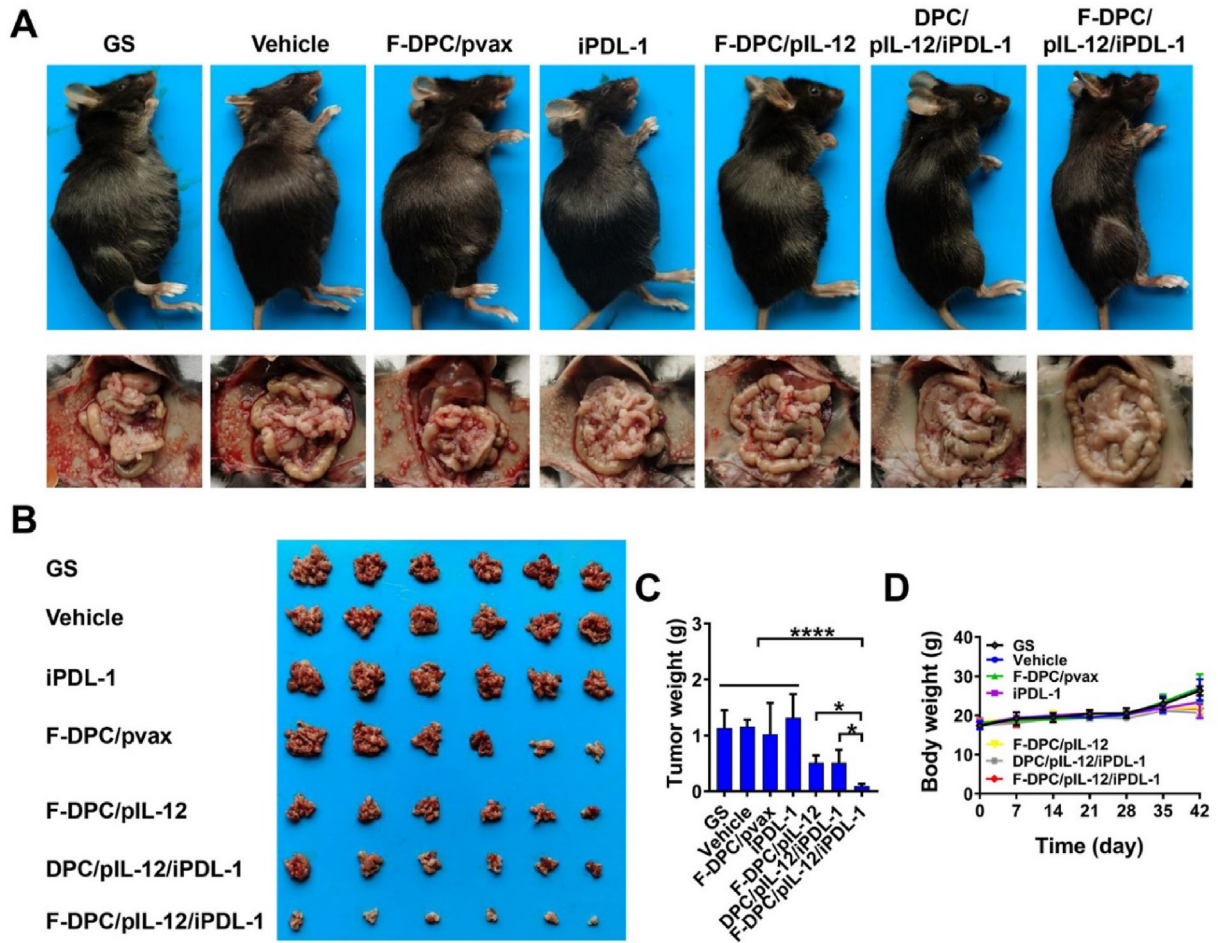

Figure 7 Therapeutic effect of F-DPC/pIL-12/iPDL-1 in ID8 peritoneal dissemination model of ovarian cancer. (A) The tumor burden of mice and representative images of the peritoneal cavity of mice. (B) Images of corresponding abdominal tumors. (C) Tumor weights. (D) Body weight curves. Data are presented as mean ± SEM ($n = 6$). *$P < 0.05$; ****$P < 0.0001$.
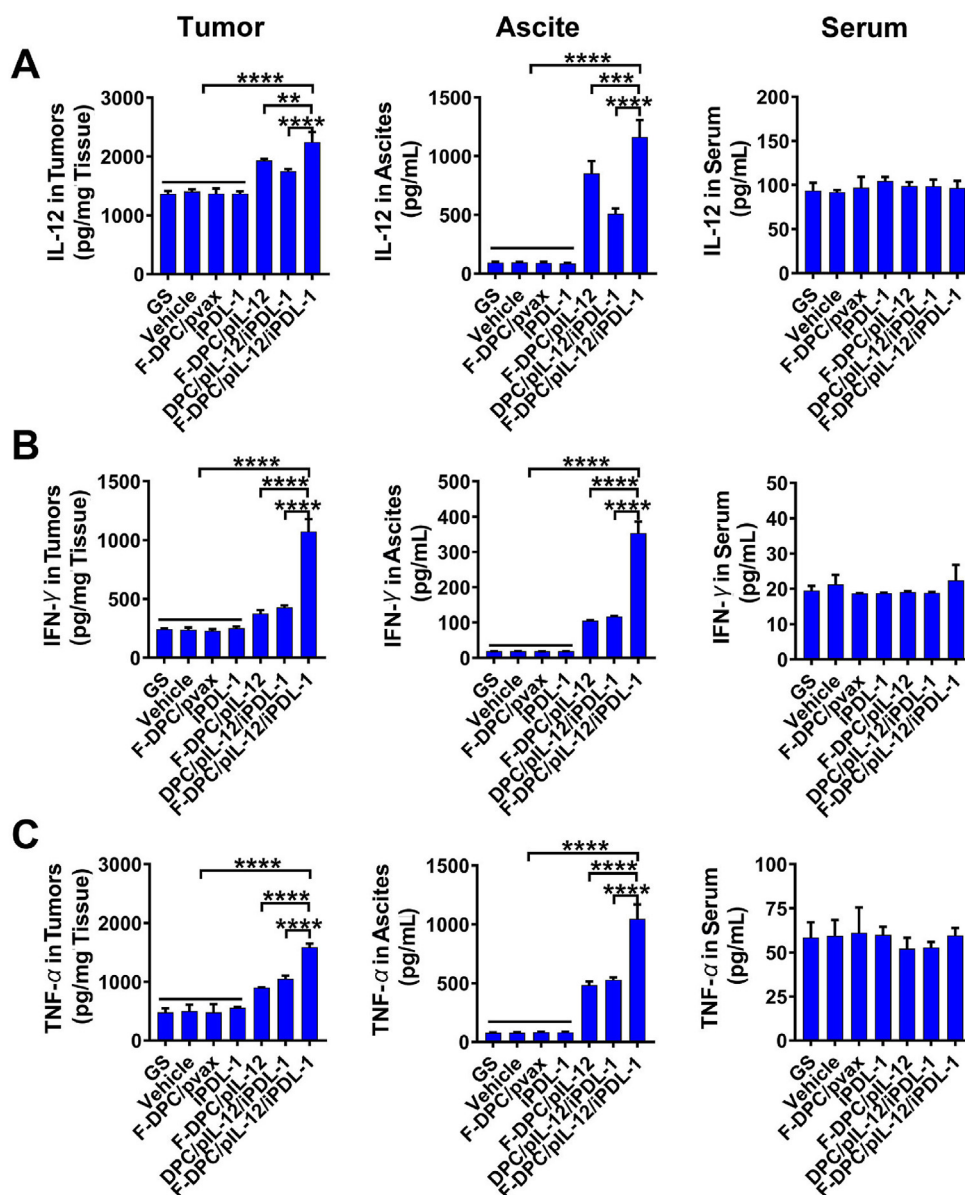
Figure 8 F-DPC/pIL-12/iPDL-1 treatment increased the expression of IL-12, IFN-γ and TNF-α *in vivo*. Tumor tissues, ascites and serums were collected after different treatments with GS, F-DPC (vehicle), F-DPC/pvax, iPDL-1, F-DPC/pIL-12, DPC/pIL-12/iPDL-1 and F-DPC/pIL-12/iPDL-1, and the expressions of IL-12 (A), IFN-γ (B) and TNF-α (C) in tumor tissues, ascites and serums were detected by ELISA. Data are presented as mean ± SEM (n = 3). **$P < 0.01$, ***$P < 0.001$, ****$P < 0.0001$).

results showed increased lymphocyte viability in the F-DPC/pIL-12/iPDL-1, DPC/pIL-12/iPDL-1 and F-DPC/pIL-12 treatment groups, among which, the effect in F-DPC/pIL-12/iPDL-1 treatment group was very significant (Fig. 6A). Then, ID8 cells were incubated with the supernatant of stimulated lymphocytes and it was shown that the viability of ID8 cells in F-DPC/pIL-12/iPDL-1, DPC/pIL-12/iPDL-1, and F-DPC/pIL-12 treated groups were all inhibited, with viability in the F-DPC/pIL-12/iPDL-1 treated group being the lowest (Fig. 6B), indicating that the combination of pIL-12 and iPDL-1 had a stronger inhibitory effect on tumor cells. In addition, the supernatant of ID8 cells transfected with F-DPC/pIL-12/iPDL-1 also efficiently increased the secretion of TNF-α and IFN-γ from lymphocytes (Fig. 6C and D). Moreover, microscopic observation showed that the number of lymphocytes in the F-DPC/pIL-12/iPDL-1 treatment group increased

remarkably, indicating that proliferation was significantly promoted (Fig. 6E). It was also revealed that higher percentages of CD4^{+}CD69^{+}, CD4^{+}IFN-γ^{+}, CD8^{+}CD69^{+} and CD8^{+}IFN-γ^{+} lymphocyte subsets in F-DPC/pIL-12/iPDL-1, DPC/pIL-12/iPDL-1, F-DPC/pIL-12-treated groups, with the percentage in the F-DPC/pIL-12/iPDL-1-treated group being the highest (Fig. 6F). These results jointly indicate that the combination of pIL-12 and iPDL-1 can exert a stronger stimulatory effect on lymphocytes than pIL-12 alone.

3.7. Combination therapy markedly inhibited peritoneal dissemination of ovarian cancer by reprogramming the TME

The antitumor effect of the F-DPC/pIL-12/iPDL-1 complexes in a mouse model with peritoneal ovarian cancer was invetigated.
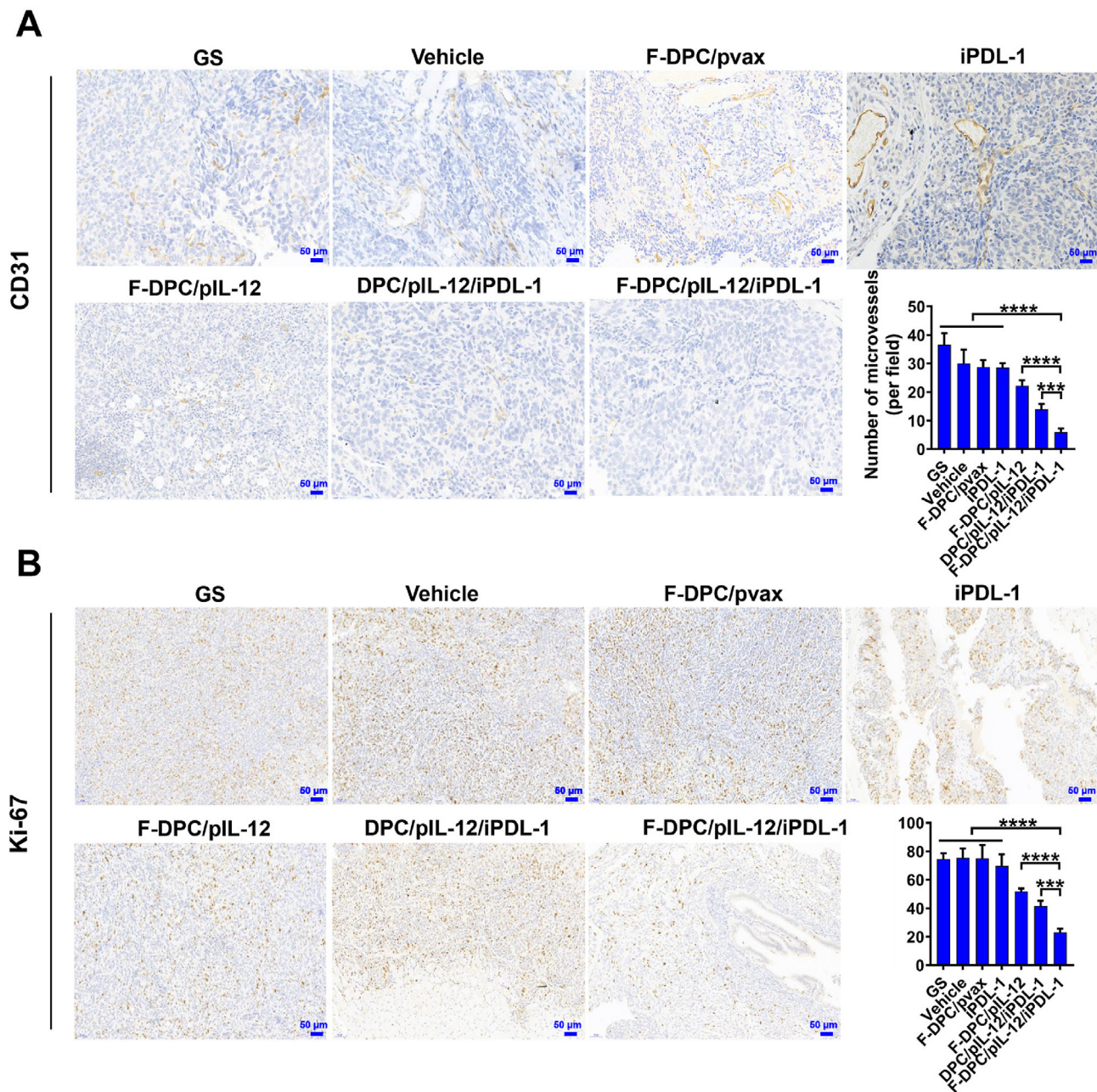
Figure 9 Representative images of the CD31 and Ki-67 staining of tumor tissues. (A) Expression of vascular endothelial marker CD31 in tumors of different treatment groups. (B) Expression of proliferative marker Ki-67 in tumors of different treatment groups. Scale bar = 50 μm. Data are presented as mean ± SEM (n = 5). ***$P < 0.001$, ****$P < 0.0001$.

Compared with GS, vehicle or F-DPC/pVAX treatment, F-DPC/pIL-12, DPC/pIL-12/iPDL-1 and F-DPC/pIL-12/iPDL-1 treatment significantly inhibited tumor dissemination in ovarian cancer mouse models (Fig. 7A and B). F-DPC/pIL-12, DPC/pIL-12/iPDL-1 and F-DPC/pIL-12/iPDL-1 treated groups showed an obvious reduction in average tumor weight but no significant change in body weight (Fig. 7C and D). Moreover, the F-DPC/pIL-12/iPDL-1 treatment had more significant antitumor effects compared with the F-DPC/pIL-12 and DPC/pIL-12/iPDL-1 treatments, indicating that the F-DPC complexes delivering both pIL-12 and iPDL-1 exerted the strongest anti-tumor effect in ovarian cancer treatment. Then, we investigated the targeted delivery capability of the F-DPC/pIL-12/iPDL-1 complexes *in vivo*

and its remodeling effect on ovarian cancer TME. The expression levels of IL-12 in tumors and ascites were increased in the F-DPC/pIL-12, DPC/pIL-12/iPDL-1 and F-DPC/pIL-12/iPDL-1 groups, and the expression was highest in the F-DPC/pIL-12/iPDL-1 group (Fig. 8A). It was also disclosed that there was no significant difference in the serum levels of IL-12 among different groups. These results indicate that the F-DPC complexes delivering pIL-12 could achieve high expression of IL-12 in tumor sites, and in combination with iPDL-1 can synergistically upregulate the expression of IL-12 at the tumor site. In addition, the F-DPC/pIL-12 DPC/pIL-12/iPDL-1 and F-DPC/pIL-12/iPDL-1 groups also had significantly upregulated secretion of the anti-tumor cytokines such as IFN-γ and TNF-α in tumor sites and ascites in ovarian

cancer models (Fig. 8B and C), with the secretion level in the F-DPC/pIL-12/iPDL-1 group being the highest. However, there was no significant change in the expression of IFN-γ and TNF-α in the serum of each treatment group, indicating that F-DPC/pIL-12/iPDL-1 treatment led to higher local concentrations of immunostimulating effectors IFN-γ and TNF-α in tumor tissues, while reducing the potential systemic inflammatory response. The above results demonstrate the excellent tumor-targeting ability of the F-DPC/pIL-12/iPDL-1 complexes.

The effects of pIL-12 and iPDL-1 combined immunotherapy on immune cell infiltration in TME were studied in the research. Results showed that DPC/pIL-12/iPDL-1 or F-DPC/pIL-12/iPDL-1 treatment significantly increased the intratumoral infiltration of CD4$^+$CD69$^+$, CD8$^+$CD69$^+$, CD4$^+$IFN-γ^+, and CD8$^+$IFN-γ^+ cell subsets (Supporting Information Fig. S4−S7). NK cells can directly kill tumor cells and also secret various cytokines, chemokines and growth factors to activate other immune cells, and increased intratumoral infiltration of NK cells is correlated with a better prognosis[54]. Our results showed a remarkable increase in CD49b$^+$CD107a$^+$ cell subsets in ascites of the DPC/pIL-12/iPDL-1 and F-DPC/pIL-12/iPDL-1 treatment groups (Supporting Information Fig. S8). In addition, the F-DPC/pIL-12/iPDL-1 treatment group showed the highest proportion of CD49b$^+$CD107a$^+$ cell subset in the spleen compared with that in the DPC/pIL-12/iPDL-1 treatment group, indicating that F-DPC/pIL-12/iPDL-1 could promote the activation of NK cells more significantly (Supporting Information Fig. S9). Taken together, the antitumor effect of F-DPC/pIL-12/iPDL-1 may be related to the enhancement of antitumor immunity by promoting the activation of NK cells in spleen and tumor site.

3.8. F-DPC/pIL-12/iPDL-1 suppressed tumor angiogenesis and proliferation with low toxicity

Furthermore, we examined tumor vascular proliferation and tumor cell proliferation by CD31 staining and Ki-67 staining assays, respectively. Results showed that the F-DPC/pIL-12/iPDL-1 treatment group exerted the most potent anti-angiogenic effect and anti-proliferative effect indicated by the fewest Ki67 positive ratio and microvessel density (Fig. 9). These suggested that F-DPC/pIL-12/iPDL-1 can effectively reduce tumor angiogenesis and inhibit tumor cell proliferation. For evaluating the safety of F-DPC/pIL-12/iPDL-1 treatment on ovarian cancer-bearing mice, H&E staining of vital organs (heart, liver, spleen, lung and kidney) in each treatment group was performed, which showed no obvious pathological changes or inflammatory infiltration in each treatment group (Supporting Information Fig. S10). In addition, no significant changes in liver function indexes, kidney function indexes and lipid index, and the relevant serum markers were within the normal ranges (Supporting Information Fig. S11). Preliminary safety evaluation results indicated that immunogene therapy with F-DPC/pIL-12/iPDL-1 complexes was well tolerated in mice with no obvious systemic toxicity.

In summary, F-DPC/pIL-12/iPDL-1 complexes exhibited significant anti-tumor effects in ovarian cancer both *in vitro* and *in vivo*. The possible mechanism is the remodeling the TME of ovarian cancer, which enhances the activation of anti-tumor immunity and alleviates immunosuppression. Specifically, it can promote T lymphocytes activation, increase cytotoxic T cells infiltration into the tumor, promote maturation of DCs, inhibit macrophage polarization toward M2 phenotype, and promote infiltration of NK cells into the tumor site. Our results showed that F-DPC/pIL-12/iPDL-1 treatment significantly increased the number

of activated CD4$^+$ and CD8$^+$ T cells compared to F-DPC/pIL-12 or iPDL-1 alone, suggesting that the combination of the two immunotherapeutic agents could significantly promote cytotoxic T cell activation and increase their intratumor infiltration. F-DPC/pIL-12/iPDL-1 also significantly increases the expression of co-stimulatory molecules like CD80, CD86 and MHCII in DCs, indicating improved maturation of DCs and and subsequently leading to enhancement in T cell-mediated anti-tumor immunity. Moreover, we found that F-DPC/pIL-12/iPDL-1 distinctively promoted the activation of STAT1 pathway, restraining the polarization of macrophages toward the M2 phenotype, and significantly increase CD49b and CD107a expression in splenic and intratumoral NK cells, indicating enhanced natural killer cell activity. Furthermore, it can significantly upregulate the secretion levels of pro-inflammatory cytokines such as IFN-γ and TNF-α to enhance antitumor immune effects. Taken together, our results proved that the F-DPC/pIL-12/iPDL-1 complexes can effectively enhance immune activation and improve the immunosuppressive state of TME, and finally play a strong specific anti-tumor immune effect.

4. Conclusions

In this study, a novel FR-targeted non-viral vector system-F-DPC is designed to achieve efficient delivery of pIL-12 and small molecule iPDL-1, which actively targets ovarian cancer and displays impressive immunomodulatory and anti-tumor effects. Our results show that F-DPC/pIL-12/iPDL-1 complex is more powerful to activate T lymphocytes, inhibit macrophage M2 polarization, increase DCs cells maturation, and promote NK cells activation in TME than DPC/pIL-12/iPDL-1. Moreover, it is validated that F-DPC/pIL-12/iPDL-1 combination therapy exhibits superior anti-tumor effect in mice model of abdominal ovarian cancer, with neovascularization and tumor proliferation inhibited markedly without obvious systemic toxicity. In conclusion, the treatment strategy of FR-targeted delivery of immunostimulating gene and checkpoint blocker based on F-DPC nanoparticles shows great application potential and might be a promising option for ovarian cancer therapy.

Author contributions

Yunzhu Lin, Xiang Wang, Shi He and Zhongxin Duan participated in the implementation of the experiment. Yunchu Zhang carried out data processing and analysis. Xiaodong Sun, Yuzhu Hu and Yuanyuan Zhang participated in the study design and revised the manuscript. Zhiyong Qian, Xiang Gao, Zhirong Zhang conceived and supervised the work. All authors have discussed and approved the manuscript.

Conflicts of interest

The authors declare that they have no known competing financial interests or personal relationships that could have appeared to influence the work reported in this paper.

Appendix A.   Supporting information

Supporting data to this article can be found online at https://doi.org/10.1016/j.apsb.2023.08.014.

References

1. Torre LA, Trabert B, DeSantis CE, Miller KD, Samimi G, Runowicz CD, et al. Ovarian cancer statistics. 2018. *CA A Cancer J Clin* 2018;**68**:284−96.

2. Miller KD, Nogueira L, Devasia T, Mariotto AB, Yabroff KR, Jemal A, et al. Cancer treatment and survivorship statistics. 2022. *CA A Cancer J Clin* 2022;**72**:409−36.

3. Sung H, Ferlay J, Siegel RL, Laversanne M, Soerjomataram I, Jemal A, et al. Global cancer statistics 2020: GLOBOCAN estimates of incidence and mortality worldwide for 36 cancers in 185 countries. *CA A Cancer J Clin* 2021;**71**:209−49.

4. Kuroki L, Guntupalli SR. Treatment of epithelial ovarian cancer. *BMJ* 2020:371.

5. Gardner GJ, Chi DS. Recurrent ovarian cancer—sculpting a promising future with surgery. *N Engl J Med* 2021;**385**:2187−8.

6. Chen SQ, Xie P, Cowan M, Huang H, Cardenas H, Keathley R, et al. Epigenetic priming enhances antitumor immunity in platinum-resistant ovarian cancer. *J Clin Invest* 2022;**132**:e158800.

7. Hamilton PT, Anholt BR, Nelson BH. Tumour immunotherapy: lessons from predator-prey theory. *Nat Rev Immunol* 2022;**22**:765−75.

8. Chen C, Ke JY, Zhou XE, Yi W, Brunzelle JS, Li J, et al. Structural basis for molecular recognition of folic acid by folate receptors. *Nature* 2013;**500**:486−9.

9. Han SY, Wu J. Three-dimensional (3D) scaffolds as powerful weapons for tumor immunotherapy. *Bioact Mater* 2022;**17**:300−19.

10. Liu XX, Gao X, Zheng SP, Wang BL, Li YY, Zhao CJ, et al. Modified nanoparticle mediated IL-12 immunogene therapy for colon cancer. *Nanomedicine* 2017;**13**:1993−2004.

11. Glassman CR, Mathiharan YK, Jude KM, Su L, Panova O, Lupardus PJ, et al. Structural basis for IL-12 and IL-23 receptor sharing reveals a gateway for shaping actions on T *versus* NK cells. *Cell* 2021;**184**:983−99.

12. Mansurov A, Ishihara J, Hosseinchi P, Potin L, Marchell TM, Ishihara A, et al. Collagen-binding IL-12 enhances tumour inflammation and drives the complete remission of established immunologically cold mouse tumours. *Nat Biomed Eng* 2020:531−43.

13. Xu CX, Zhang YP, Rolfe PA, Hernandez VM, Guzman W, Kradjian G, et al. Combination therapy with NHS-muIL12 and avelumab (anti-PD-L1) enhances antitumor efficacy in preclinical cancer models. *Clin Cancer Res* 2017;**23**:5869−80.

14. Asteamezaga M, Dandrea A, Kubin M, Trinchieri G. Cooperation of natural killer cell stimulatory factor/interleukin-12 with other stimuli in the induction of cytokines and cytotoxic cell-associated molecules in human T and NK cells. *Cell Immunol* 1994;**156**:480−92.

15. Kaczanowska S, Beury DW, Gopalan V, Tycko AK, Qin HY, Clements ME, et al. Genetically engineered myeloid cells rebalance the core immune suppression program in metastasis. *Cell* 2021;**184**:2033−52.

16. Voest EE, Kenyon BB, Oreilly MS, Truitt G, Damato RJ, Folkman J. Inhibition of angiogenesis *in vivo* by interleukin 12. *J Natl Cancer Inst* 1995;**87**:581−6.

17. Del Vecchio M, Bajetta E, Canova S, Lotze MT, Wesa A, Parmiani G, et al. Interleukin-12: biological properties and clinical application. *Clin Cancer Res* 2007;**13**:4677−85.

18. Mansurov A, Hosseinchi P, Chang K, Lauterbach AL, Gray LT, Alpar AT, et al. Masking the immunotoxicity of interleukin-12 by fusing it with a domain of its receptor *via* a tumour-protease-cleavable linker. *Nat Biomed Eng* 2022;**6**:819−29.

19. Xue DY, Moon B, Liao J, Guo JY, Zou ZZ, Han YF, et al. A tumor-specific pro-IL-12 activates preexisting cytotoxic T cells to control established tumors. *Sci Immunol* 2022;**7**:eabi6899.

20. Barberio AE, Smith SG, Correa S, Nguyen C, Nhan B, Melo M, et al. Cancer cell coating nanoparticles for optimal tumor-specific cytokine delivery. *ACS Nano* 2020;**14**:11238−53.

21. Barberio AE, Smith SG, Pires IS, Iyer S, Reinhardt F, Melo MB, et al. Layer-by-layer interleukin-12 nanoparticles drive a safe and effective response in ovarian tumors. *Bioeng Transl Med* 2023;**8**:e10453.

22. Sun LJ, Kees T, Almeida AS, Liu BD, He XY, Ng D, et al. Activating a collaborative innate-adaptive immune response to control metastasis. *Cancer Cell* 2021;**39**:1361−74.

23. Leonard JP, Sherman ML, Fisher GL, Buchanan LJ, Larsen G, Atkins MB, et al. Effects of single-dose interleukin-12 exposure on interleukin-12-associated toxicity and interferon-gamma production. *Blood* 1997;**90**:2541−8.

24. Melero I, Mazzolini G, Narvaiza I, Qian C, Chen LP, Prieto J. IL-12 gene therapy for cancer: in synergy with other immunotherapies. *Trends Immunol* 2001;**22**:113−5.

25. Vazquez-Garcia I, Uhlitz F, Ceglia N, Lim JLP, Wu M, Mohibullah N, et al. Ovarian cancer mutational processes drive site-specific immune evasion. *Nature* 2022;**612**:778−86.

26. Yi M, Zheng XL, Niu MK, Zhu SL, Ge H, Wu KM. Combination strategies with PD-1/PD-L1 blockade: current advances and future directions. *Mol Cancer* 2022;**21**:8.

27. Tan JZ, Liu T, Fan WZ, Wei JL, Zhu BW, Liu YF, et al. Anti-PD-L1 antibody enhances curative effect of cryoablation *via* antibody-dependent cell- mediated cytotoxicity mediating PD-L1highCD11bD cells elimination in hepatocellular carcinoma. *Acta Pharm Sin B* 2023;**13**:632−47.

28. Wu ML, Huang QR, Xie Y, Wu XY, Ma HB, Zhang YW, et al. Improvement of the anticancer efficacy of PD-1/PD-L1 blockade *via* combination therapy and PD-L1 regulation. *J Hematol Oncol* 2022;**15**:24.

29. Clark CA, Gupta HB, Sareddy G, Pandeswara S, Lao S, Yuan B, et al. Tumor-Intrinsic PD-L1 signals regulate cell growth, pathogenesis, and autophagy in ovarian cancer and melanoma. *Cancer Res* 2016;**76**:6964−74.

30. Li YM, Ye ZF, Yang HY, Xu QB. Tailoring combinatorial lipid nanoparticles for intracellular delivery of nucleic acids, proteins, and drugs. *Acta Pharm Sin B* 2022;**12**:2624−39.

31. Li YL, Maciel D, Rodrigues J, Shi XY, Tomas H. Biodegradable polymer nanogels for drug/nucleic acid delivery. *Chem Rev* 2015;**115**:8564−608.

32. Zhang HX, You XR, Wang XJ, Cui L, Wang ZN, Xu FF, et al. Delivery of mRNA vaccine with a lipid-like material potentiates antitumor efficacy through Toll-like receptor 4 signaling. *Proc Natl Acad Sci USA* 2021;**118**:e2005191118.

33. Zhou S, Huang Y, Chen Y, Liu Y, Xie L, You Y, et al. Reprogramming systemic and local immune function to empower immunotherapy against glioblastoma. *Nat Commun* 2023;**14**:435.

34. Jhunjhunwala S, Hammer C, Delamarre L. Antigen presentation in cancer: insights into tumour immunogenicity and immune evasion. *Nat Rev Cancer* 2021;**21**:298−312.

35. Sanmamed MF, Chen LP. A paradigm shift in cancer Immunotherapy: from enhancement to normalization. *Cell* 2018;**175**:313−26.

36. Fernandez M, Javaid F, Chudasama V. Advances in targeting the folate receptor in the treatment/imaging of cancers. *Chem Sci* 2018;**9**:790−810.

37. Scaranti M, Cojocaru E, Banerjee S, Banerji U. Exploiting the folate receptor alpha in oncology. *Nat Rev Clin Oncol* 2020;**17**:349−59.

38. Song XR, Liu C, Wang N, Huang H, He SY, Gong CY, et al. Delivery of CRISPR/Cas systems for cancer gene therapy and immunotherapy. *Adv Drug Deliv Rev* 2021;**168**:158−80.

39. Li J, Du YT, Su HT, Cheng SX, Zhou YX, Jin YG, et al. Interfacial properties and micellization of triblock poly(ethylene glycol)-poly(epsilon-caprolactone)-polyethyleneimine copolymers. *Acta Pharm Sin B* 2020;**10**:1122−33.

40. Propper DJ, Balkwill FR. Harnessing cytokines and chemokines for cancer therapy. *Nat Rev Clin Oncol* 2022;**19**:237−53.

41. Cirella A, Luri-Rey C, Trani CAD, Teijeira A, Olivera I, Bolanos E, et al. Novel strategies exploiting interleukin-12 in cancer immunotherapy. *Pharmacol Ther* 2022;**239**:108189.

42. Zhang L, Morgan RA, Beane JD, Zheng ZL, Dudley ME, Kassim SH, et al. Tumor-infiltrating lymphocytes genetically engineered with an inducible gene encoding interleukin-12 for the immunotherapy of metastatic melanoma. *Clin Cancer Res* 2015;**21**: 2278−88.

43. Qiu NS, Wang GW, Wang JQ, Zhou Q, Guo MY, Wang YL, et al. Tumor-associated macrophage and tumor-cell dually transfecting polyplexes for efficient interleukin-12 cancer gene therapy. *Adv Mat* 2021; **33**:e2100137.

44. Kang L, Gao ZG, Huang W, Jin MJ, Wang QM. Nanocarrier-mediated co-delivery of chemotherapeutic drugs and gene agents for cancer treatment. *Acta Pharm Sin B* 2015;**5**:169−75.

45. Matulonis UA, Lorusso D, Oaknin A, Pignata S, Dean A, Denys H, et al. Efficacy and safety of mirvetuximab soravtansine in patients with platinum-resistant ovarian cancer with high folate receptor alpha expression: results from the SORAYA study. *J Clin Oncol* 2023;**41**: 2436−45.

46. "Significant activity" for ADC in ovarian cancer. *Cancer Discov* 2021; **11**:OF3.

47. Hu Y, Liu X, Ran M, Yang T, Li T, Wu Y, et al. Simultaneous delivery of immune stimulatory gene and checkpoint blocker *via* targeted nanoparticles to strengthen antitumor immunity. *Mat Today Nano* 2022;**17**:100151.

48. Li CZ, You XR, Xu X, Wu BH, Liu YY, Tong T, et al. A metabolic reprogramming amino acid polymer as an immunosurveillance activator and leukemia targeting drug carrier for T-cell acute lymphoblastic leukemia. *Adv Sci* 2022;**9**:e2104134.

49. Wojno EDT, Hunter CA, Stumhofer JS. The immunobiology of the interleukin-12 family: room for discovery. *Immunity* 2019;**50**:851−70.

50. Shan X, Hu PH, Ni LN, Shen L, Zhang YA, Ji ZM, et al. Serine metabolism orchestrates macrophage polarization by regulating the IGF1-p38 axis. *Cell Mol Immunol* 2022;**19**:1263−78.

51. Geissmann F, Manz MG, Jung S, Sieweke MH, Merad M, Ley K. Development of monocytes, macrophages, and dendritic cells. *Science* 2010;**327**:656−61.

52. Chan SH, Perussia B, Gupta JW, Kobayashi M, Pospisil M, Young HW, et al. Induction of interferon gamma production by natural killer cell stimulatory factor: characterization of the responder cells and synergy with other inducers. *J Exp Med* 1991;**173**:869−79.

53. Kobayashi M, Fitz L, Ryan M, Hewick RM, Clark SC, Chan S, et al. Identification and purification of natural killer cell stimulatory factor (NKSF), a cytokine with multiple biologic effects on human lymphocytes. *J Exp Med* 1989;**170**:827−45.

54. Shimasaki N, Jain A, Campana D. NK cells for cancer immunotherapy. *Nat Rev Drug Discov* 2020;**19**:200−18.